Time-resolved photon emission from layered turbid media

Andreas H. Hielscher, Hanli Liu, Britton Chance, Frank K. Tittel, and Steven L. Jacques

We present numerical and experimental results of time-resolved emission profiles from various layered turbid media. Numerical solutions determined by time-resolved Monte Carlo simulations are compared with measurements on layered-tissue phantoms made from gelatin. In particular, we show that in certain cases the effects of the upper layers can be eliminated. As a practical example, these results are used to analyze *in vivo* measurements on the human head. This demonstrates the influence of skin, skull, and meninges on the determination of the blood oxygenation in the brain.

Key words: Diffusion theory, photon migration, scattering, time-resolved, photon counting, reflectance, multilayer, Monte Carlo simulation, tissue phantom, blood oxygenation, brain.

1. Introduction

A. Motivation

Most biological tissues consist of layers that have different optical properties. A few examples are skin, esophagus, stomach, intestine, and bladder. These layers can be as thin as a few micrometers, such as the endothelial cell layer that covers the interior of arteries, and as thick as a centimeter, such as the skull that encapsulates the brain. An understanding of how light propagates in such layered systems is a prerequisite for any light-based therapy or diagnostic scheme. For example, different methods that use measurements of continuous-light, time- or frequency-resolved reflectance have been used to determine the blood-oxygenation status of the brain.[1–3] However, little attention has been paid to the fact that the brain is actually encapsulated by the skin, the skull, and the meninges, which are tissues with very different optical properties. The arachnoid, a substructure of the meninges, is almost free of photon absorption and scattering. On the other hand, the capillary bed in the gray matter has a high content of strongly absorbing blood. How these layers with strongly varying optical properties influence the determination of the blood oxygenation of the brain tissue has not yet been studied in detail, to our knowledge.

B. Previous Works of Other Groups

Several groups have investigated the photon migration in layered systems when light is injected continuously into the tissue. In 1979, Takatani and Graham[4] first presented theoretical results based on diffusion theory for the steady-state diffuse reflectance from a two-layer system. They also reported experimental findings from a homogenized canine gut mucosa. Keijzer *et al.*[5] approached the problem of layers with different refractive indices. For these systems, they solved the diffusion equation together with its boundary conditions by using a finite-element method. Nossal *et al.*[6] developed a three-dimensional lattice random-walk algorithm to study systems whose top layer has either a higher or lower absorption coefficient than the underlying medium. Taitelbaum *et al.*[7] used Nossal *et al.*'s results to propose an approximated theory of photon migration in a two-layered medium. Recently Schmitt *et al.*[8] generalized the approach of Takatani and Graham[4] to a multilayer model of photon diffusion in skin by including reflections from boundaries. Schmitt *et*

When this research was done, A. H. Hielscher and F. K. Tittel were with the Department of Electrical and Computer Engineering, Rice University, 6100 South Main, Houston, Texas 77251-1892; H. Liu and B. Chance are with the Department of Biochemistry and Biophysics, University of Pennsylvania, D501 Richards Building, Philadelphia, Pennsylvania 19104-6089. S. J. Jacques is with the Laser Biology Research Laboratory, Box 17, The University of Texas M.D. Anderson Cancer Center, 1515 Holcombe Boulevard, Houston, Texas 77030. A. H. Hielscher is now with the Los Alamos National Laboratory, Biotechnology Group, CST-4, MS E535, Los Alamos, New Mexico 87545.

Received 13 January 1995; revised manuscript received 11 July 1995.

0003-6935/96/040719-10$06.00/0

al. supported their findings with measurements on tissue phantoms made of gelatin with diluted milk and various dyes. Finally, Cui and Ostrander[9] developed a three-dimensional photon-diffusion finite-difference model to study steady-state photon migration in layered tissues. They suggested that the optical properties of the subdermal tissue can be determined by reflectance measurements because the effect of the upper skin layers can be eliminated.

C. Content and Structure of Our Study

We present here the numerical and the experimental results of time-resolved emission profiles from various layered media. Numerical solutions determined by time-resolved Monte Carlo simulations are compared with measurements on layered-tissue phantoms made from gelatin.

First we briefly review the principles of time-resolved reflectance methods. Subsequently we investigate simple layered structures consisting of a surface layer whose absorption coefficient differs from that of the underlying medium. The results for the time-resolved reflectance are compared with the existing steady-state studies of Nossal *et al.*[6] and Cui and Ostrander.[9] The findings from the elementary two-layer system are generalized to multilayer systems, and the influence of changes in scattering coefficients is discussed. As a practical example, *in vivo* measurements on the human head are analyzed based on the conclusions of this study; this illustrates the influence of the skin, skull, and meninges on the determination of the blood oxygenation in the brain.

2. Time-Resolved Reflectance

Time-resolved reflectance measurements can be used to determine the absorption (μ_a) and reduced scattering coefficient (μ_s') of tissues.[10,11] With this technique, a picosecond pulsed light source is used as an input signal and the reflectance is measured as a function of time at a distance of a few centimeters away from the source. Once the time-resolved signal has been obtained, there are several ways to extract the optical properties of the medium. The most accurate one is to compare the experimental data with results from Monte Carlo simulations.[11–13] However, Monte Carlo simulations are very time consuming. Consequently analysis using an iterative algorithm that compares simulation results with measurements may require several days, a time period that is usually too long in a clinical environment. A much faster way to determine the absorption and scattering coefficient is to fit a diffusion-theory curve to the data. When a semi-infinite medium is assumed and the zero-boundary condition is applied, the reflectance R measured at a source–detector separation r and time t is given by[10]

$$R(r, t) = (4\pi cD)^{-3/2}(\mu_a + \mu_s')^{-1}t^{-5/2} \times \exp\left[-\frac{r^2 + (\mu_a + \mu_s')^{-2}}{4cD}\frac{1}{t}\right]\exp(-\mu_a ct), \quad (1)$$

where $\mu_s' = \mu_s(1 - g)$ is the reduced scattering coefficient and g is the anisotropy parameter of the medium. In general g can be used to obtain values between -1 and 1. Isotropic scattering is described by $g = 0$, whereas pure backscattering gives $g = -1$ and pure forward scattering gives $g = 1$. Biological tissues usually have g values larger than 0.8. Furthermore, Eq. (1) contains the diffusion coefficient $D = [3(\mu_a + \mu_s')]^{-1}$ and the speed of light in the medium c. Taking the natural logarithm on both sides of Eq. (1) and assuming that $r \gg (\mu_a + \mu_s')^{-1}$ yields

$$\ln[R(r, t)] = \kappa - \frac{5}{2}\ln(t) - \left(ct + \frac{a}{t}\right)\mu_a - \left(\frac{a}{t}\right)\mu_s', \quad (2)$$

where $a = 3r^2/4c$ and $\kappa = -3/2\ln(4\pi cD) - \ln(\mu_a + \mu_s')$. Because it is extremely problematic to determine the absolute amplitude of the reflectance signal in time-resolved experiments, the μ_s' and μ_a dependence of κ should be ignored, and κ should be treated as an independent fitting parameter. This also has the advantage that Eq. (2) is linear with respect to the optical properties μ_a and μ_s'. Simple and fast mean-least-squares fitting algorithms can be implemented to determine μ_a and μ_s' from a given data set. Furthermore, Eq. (2) shows that the reduced scattering coefficient μ_s', which is usually much larger than μ_a, dominates the behavior of the reflectance signal for $t \ll a\mu_s'$. For $t \gg a\mu_s$'s, on the other hand, μ_a has the strongest influence.

It has to be emphasized that the expression given in Eq. (2) is derived for a semi-infinite and homogeneous medium with the so-called zero-boundary condition. In medical situations, such media are not actually encountered. The semi-infinite approximation is acceptable, though, because for all practical purposes significant contribution to measurements comes from only a few centimeters around the source.

On the other hand, the assumption of homogeneity does not in general hold, as already mentioned in Section 1. However, Eq. (2) is used in our study to determine what we call apparent absorption and apparent scattering coefficients of heterogeneous media. Although the principal composition of the tissues under investigation is usually known, details such as the exact layer thickness and optical properties of the tissue are often unknown. It thus seems practical to treat the tissue as a black box and to apply a simple theory with a few variables. As this study shows, the concept of apparent optical properties can yield useful information in a lot of cases.

The assumption of a zero-boundary condition has been found to yield scattering and absorption coefficients from experimental data with almost the same accuracy as the more sophisticated approaches when extrapolated-boundary or partial-current-boundary conditions are assumed.[13] Thus it seems unnecessary to apply more complex nonlinear-fitting algo-

rithms as required when extrapolated-boundary or partial-current-boundary conditions are used.

3. Layered Media with Absorption Changes

A. Introduction

In this section we address the problem of a surface layer whose absorption differs from that of the underlying medium. The scattering coefficient is kept constant for both layers. Two cases are investigated: a high-absorbing medium on top of an underlying low-absorbing material and vice versa. The results found for these two basic tissue structures can be generalized to more complex multilayered media, which are discussed in Section 5.

B. Methods

For studying layered tissue structures, a time-resolved Monte Carlo code was developed.[14,15] As input parameters one can choose the optical properties (μ_a, μ_s, g, n), layer thickness, source and detector type, source–detector separation, and number of photons. For the simulations presented here a δ-function pulse was inserted into various semi-infinite layered media. The reflectance $R(r, t)$ (in inverse square millimeters times inverse nanoseconds) was recorded as a function of the source–detector separation r and time t. The spatial resolution was 1 mm over a total distance of 4 cm. The time resolution was chosen to be 10 ps over a total time of 2.56 ns, giving 256 data points. If not stated otherwise, 2,000,000 photons were used for a simulation, and the reference index was set to 1.37. The Monte Carlo model accounted for the index mismatch at the air–tissue boundary by calculating the Fresnel reflection.[14] Further details concerning the code as well as results on semi-infinite homogeneous media can be found elsewhere.[11,13–17]

The simulation results were tested experimentally on layered-tissue phantoms. These phantoms were made out of collagen gelatin made from porcine skin (Sigma, Type A, 300 Bloom). TiO_2 powder (Sigma) was added to the gelatin to introduce scatterers into the medium. Sizes of the TiO_2 particles were Gaussian distributed with a mean size of 280 μm and a full width at half-maximum of 80 μm. India ink in different concentrations served as absorber. Gels with different optical properties were stacked on top of each other to yield a layered-tissue structure. The optical properties of the different layers were determined by time-resolved reflectance measurements on homogeneous samples that were made of the same material as the layers. To simulate semi-infinite media, large 15 cm × 15 cm × 15 cm samples were used for these measurements.

As light sources for the time-resolved reflectance measurements, laser diodes were used that were driven by a picosecond light pulser (PLP-02, Hamamatsu Photonics K.K., Hamamatsu, Japan). Light pulses with a duration of 10–50 ps (full width at half-maximum) were emitted at a repetition rate of 10 MHz. The peak power reached ~100 mW for the wavelength of 780 nm. The light was guided through a 200-μm input fiber to the surface of the tissue or tissue model. The scattered photons were collected with a fiber bundle of 3-mm diameter that was placed in contact with the surface at a distance d from the input fiber. Through the fiber bundle the photons were guided to a microchannel plate photomultiplier.

For the detection a standard time-correlated single-photon-counting method was used.[18] The system was able to detect up to 10^5 photons per second, which were distributed over 256 channels with a width of approximately 20 ps. The single-photon-counting data were corrected by deconvolution with the normalized instrument function. Through multiple measurements on various test samples, we found that the standard deviation s, given in percentage of photon counts N in a given channel, can be approximated by $s = 300/\sqrt{N}\,(\%)$. A more detailed description of the experimental setup can be found elsewhere.[19]

C. High-Absorbing Layer on Low-Absorbing Medium

1. Monte Carlo Simulations

The first case of a two-component structure is a layer of high-absorbing material placed on a low-absorbing medium. A practical example is the skin on top of the skull. Figure 1 shows a time-resolved Monte Carlo simulation of two homogeneous media (I) and (II) and one layered medium (III) that is a combination of (I) and (II). The 8-mm-thick upper layer has a high absorption coefficient of $\mu_a = 0.2\ \mathrm{cm}^{-1}$. The underlying bulk material has an absorption coefficient that is 20-fold lower ($\mu_a = 0.01\ \mathrm{cm}^{-1}$) than that of the upper layer. The scattering is the same in both media ($\mu_s = 50\ \mathrm{cm}^{-1}$, $g = 0.9$, $\mu_s' = 5\ \mathrm{cm}^{-1}$). The refractive indices of the media are set to $n = 1.37$. These optical properties were chosen to resemble typical tissue values in the near infrared.[20–23]

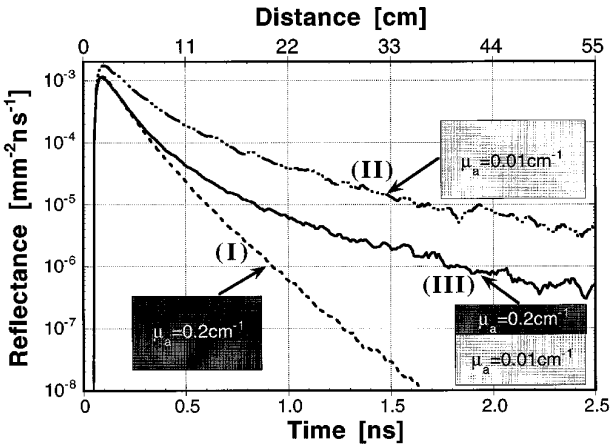

Fig. 1. Monte Carlo simulations for a two-layer system [(III)]. Both layers have the same $\mu_s' = 5\ \mathrm{cm}^{-1}$. The upper layer is 8 mm thick. The source–detector separation is 1 cm. The related homogeneous media are shown as reference [(I) and (II)].

It can be seen that time-resolved-reflectance curve (III) of the layered tissue at early times follows curve (I) of the homogeneous medium with higher absorption (Fig. 1). This means that the detected photons have traveled in only the upper layer and are not influenced by the underlying bulk material. After approximately 300 ps, curves (III) and (I) start to deviate, indicating that photons reaching the lower layer contribute to the detected signal. After ~1 ns, curve (III) of the layered medium becomes parallel to curve (II) of the homogeneous medium with the optical properties of the underlying medium. As discussed in Section 2, the absorption coefficient of a tissue mostly influences the late part of the time-resolved reflectance. Thus a fit of diffusion theory [Eq. (2)] to curve (II) of the homogeneous medium and curve (III) of the layered medium yields the same μ_a. This suggests that the absorption coefficient μ_a of the hidden tissue can be measured through the upper layer.

There is a simple explanation for this behavior. The more time that elapses, the deeper the photons penetrate into the medium. After only 1 ns, photons actually have traveled ~22 cm in the tissue. This means that most of the time a photon propagates is spent in the lower layer. The 8-mm-thick upper layer becomes optically thinner and thinner as time elapses.

This has been found to hold for even very thick top layers of up to 1.0 cm and for strong-absorbing top layers of up to $\mu_a = 1\ \text{cm}^{-1}$. An increase in the absorption of the top layer eventually leads to a total attenuation of the signal. However, as long as enough photons can be sampled, the absorption of the underlying medium can be determined.

2. *Experiments on Tissue Phantoms*

The results of the Monte Carlo simulations are confirmed experimentally, as shown in Fig. 2. In this example, the top medium has an absorption coefficient of $\mu_a = 0.50\ \text{cm}^{-1}$. The underlying gelatin has a low absorption of $0.045\ \text{cm}^{-1}$. Top layers with different thicknesses of up to 1.5 cm were placed on the low-absorbing gelatin. As can be seen in all cases, the time-resolved emission curves for the layered media follow first the curve for the high-absorbing homogeneous top layer. Depending on the layer thickness, the curves of the layered media start to deviate from the curves of the homogeneous media at times between 100 and 800 ps. For layers thicker than 1 cm, a sharp breaking point can be observed. In this case, the deviations between the homogeneous and the layered media start to appear on the decaying part of the impulse response. After a short transition time, all curves bend strongly toward the curve representative for the low-absorbing underlying homogeneous medium. Indeed, a diffusion-theory fit to data points with $t > 1$ ns yields, within 3%, the same μ_a for the curves with $d = 0$ ($\mu_a = 0.0451\ \text{cm}^{-1}$), $d = 4$ mm ($\mu_a = 0.0444\ \text{cm}^{-1}$), and $d = 8.5$ mm ($\mu_a = 0.0457\ \text{cm}^{-1}$). But, when the top layer becomes thicker than 1.1 cm, the diffusion-theory fits yield absorption coefficients that are over 10% larger than the μ_a of the underlying tissue. However, layers of that thickness are rarely encountered in biological tissues. Therefore one can summarize that for all practical purposes it is possible to determine the absorption coefficient of an underlying medium through the upper layer by fitting the late part of the time-resolved reflectance. Different thicknesses of the upper layer seem to affect only the amplitude of the signal and not the determination of the absorption coefficient of the lower layer.

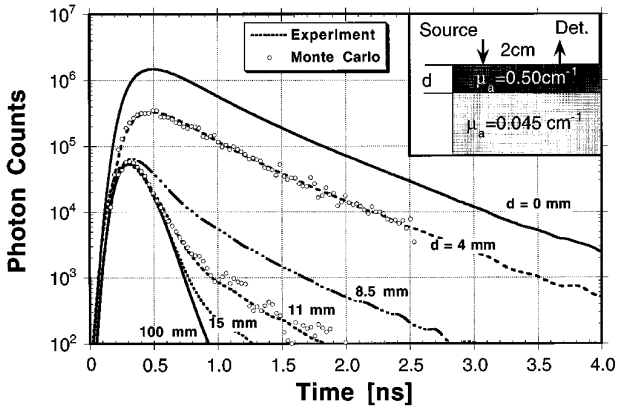

Fig. 2. Experiments on layered gel phantoms with a layer of high-absorbing gel on top of a low-absorbing gel. The values labeled along the dashed curves indicate the thicknesses of the top layer. The open circles indicate results from a Monte Carlo simulation for the layered system. The scattering coefficient μ_s' is 10.0 cm^{-1} for all media.

Besides the experimental findings, the results from two Monte Carlo simulations are displayed in Fig. 2. The simulation results were normalized to match the amplitude of the experiments. The examples show a good quantitative agreement between experiments and Monte Carlo simulations.

D. Low-Absorbing Layer on High-Absorbing Medium

1. *Monte Carlo Simulations*

The results shown in Figs. 3(a) and 3(b) are obtained for the case in which the top layer is less absorbing than the underlying medium. In both graphs, the surface layer, with a low absorption coefficient of $\mu_a = 0.01\ \text{cm}^{-1}$, is 4 mm thick, and the source–detector separation is 1 cm. In Fig. 3(a), the underlying layer has an absorption coefficient of $\mu_a = 0.2\ \text{cm}^{-1}$. Scattering is the same throughout the system ($\mu_s = 50\ \text{cm}^{-1}$, $g = 0.9$, $\mu_s' = 5\ \text{cm}^{-1}$). It can be seen that, in this case, after 1 ns the slope of the layered medium is parallel to the slope determined for the underlying homogeneous medium with the higher absorption coefficient. Thus a diffusion-theory fit to both curves (II) and (III) yields the same absorption coefficient for both systems, as already described in Subsection 3.C.

However, in contrast to the case in which the surface layer has a higher absorbance, this does not hold true if the upper layer's thickness or the lower

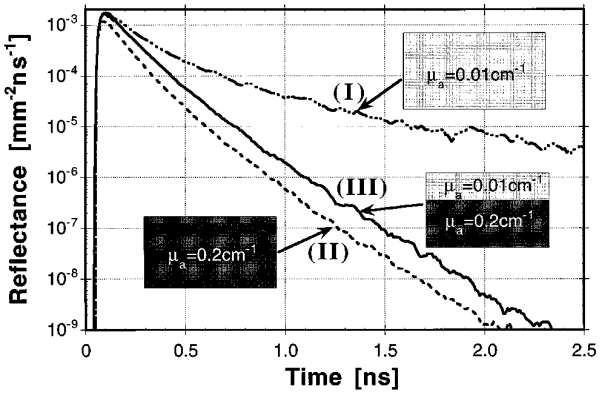

(a)

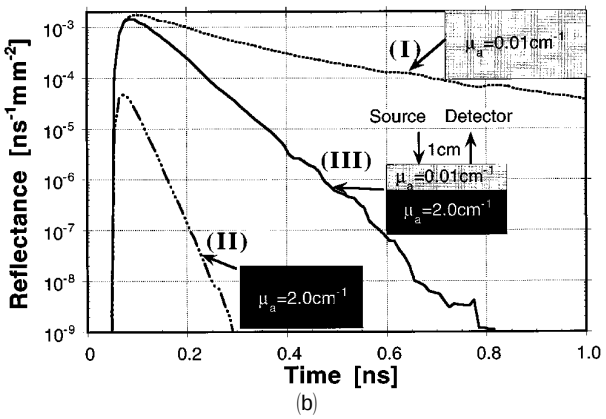

(b)

Fig. 3. Monte Carlo simulations for two-layer systems [(III)]. (a) Both layers have the same $\mu_s' = 5$ cm^{-1}. The upper layer is 4 mm thick. The source–detector separation is 1 cm. (b) All parameters are as in (a), except the absorption coefficient of the lower layer has been increased tenfold. The related homogeneous media are shown as reference [(I) and (II)].

layer's absorption coefficient is increased. In Fig. 3(b), the absorption coefficient of the lower layer has been increased 10 times to $\mu_a = 2$ cm^{-1} and is thus 200 times higher than the μ_a of the upper layer. Now the slope of the time-resolved impulse response measured on the layered system is no longer parallel to the homogeneous medium with the high absorption. Thus a diffusion-theory fit for curves (II) and (III) gives different absorption coefficients for both systems. In general, we found that in the case of a low-absorbing layer on top of a high-absorbing medium, the apparent absorption coefficient is a function of layer thickness as well as the optical properties of both layers. This is in contrast to the case in which the high-absorbing layer is on top of a low-absorbing medium. In the latter case, the apparent absorption is always given by the absorption coefficient of the underlying medium.

2. *Experiments on Tissue Phantoms*

The findings from Monte Carlo simulations were confirmed experimentally for a system whose top layer is less absorbing than the underlying medium (Fig. 4). The strongly absorbing bottom medium ($\mu_a = 0.87$ cm^{-1}) is covered with the low-absorbing

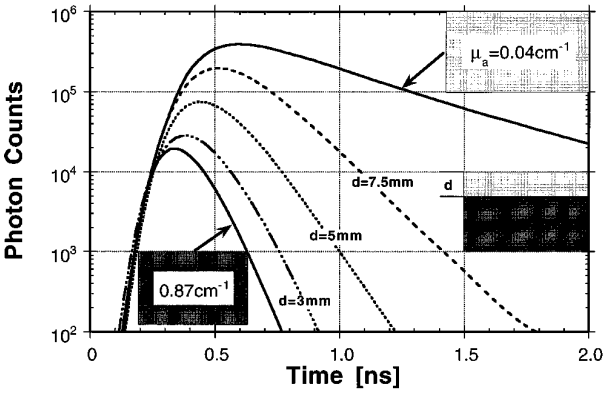

Fig. 4. Experiments on layered gel phantoms with a layer of low-absorbing gel on top of an ~22-fold more strongly absorbing gel. The values labeled along the dashed curves indicate the thicknesses of the top layer. The scattering coefficient μ_s' is 12.0 cm^{-1} for all media.

($\mu_a = 0.04$ cm^{-1}) surface layer. Increasing the thickness of the top layer yields a decreasing apparent absorption coefficient. For only the very thin layer of 3 mm is the apparent absorption coefficient close to the absorption coefficient of the bottom layer.

Figure 5 summarizes the results of 18 experiments on gel phantoms with a low-absorbing top layer. The x axis is the absorption coefficient of the underlying medium. For three different layer thicknesses, we determined the apparent absorption coefficient of the layered-tissue structure was determined by fitting Eq. (2) to the measured time-resolved reflectance curve. The source–detector separation was 2 cm. The absorption coefficient of the upper layer was $\mu_a = 0.042$ cm^{-1}. As can be seen, if the upper layer is thin (3 mm), the apparent absorption coefficient matches the absorption coefficient of the lower layer within the accuracy of the measurements up to μ_a ~0.5 cm^{-1}. As the absorption coefficient of the underlying material is further increased, the appar-

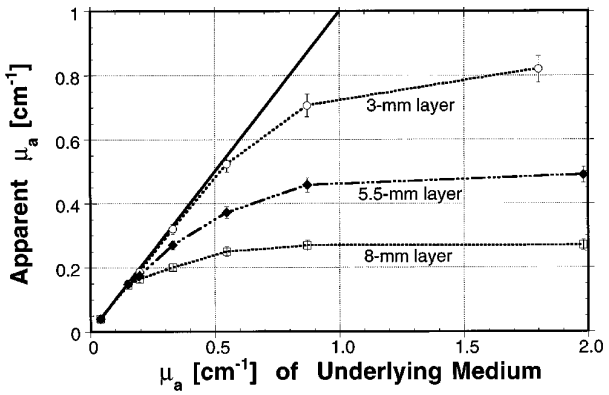

Fig. 5. Apparent absorption coefficient as a function of the absorption coefficient of the underlying medium and the layer thickness (experimental results). The low-absorbing top layer has an absorption coefficient of $\mu_a = 0.042$ cm^{-1}. The scattering coefficient is constant throughout the phantom ($\mu_s' = 10.5$ cm^{-1}). The separation between the detector and the source is 2 cm.

ent absorption coefficient underestimates the actual absorption coefficient.

When the layer thickness is increased, the deviation between the actual and the apparent absorption coefficients occurs at an even lower absorption coefficient for the bottom medium (here at approximately $\mu_a = 0.2\ \mathrm{cm}^{-1}$). If the absorption of the underlying tissue is increased beyond $\sim 1\ \mathrm{cm}^{-1}$, the system with the 8-mm layer does not show any measurable change in the apparent absorption coefficient. The top layer totally shields the information about the underlying tissue. One actually measures the reflectance from a slab with thickness d, instead of the reflectance from a semi-infinite medium.

4. Discussion

A. Time-Resolved Versus Continuous-Light Studies

Nossal *et al.*[6] reported similar differences as found in our study for the two cases of high-absorbing material on low-absorbing underlying media and vice versa. However, Nossal *et al.* investigated the photon-emission profile as a function of source–detector separation rather than of time. For the case of high-absorbing material on top of a low-absorbing medium, they reported sharp breaking points at certain separations, depending on the thickness of the top layer. After that sharp breaking point, all curves become parallel to the curve for the homogeneous medium with optical properties of the underlying medium. In the inverse case of low-absorbing material on top of a high-absorbing medium, the sharp breaking points are missing, and the slopes of the reflectance curves do not become parallel at large distances. Our study confirms the findings of Nossal *et al.;* however, in our work time takes on the role of the source–detector separation.

The advantage of using time-domain techniques lies in the fact that information from deep-lying media can be obtained with even small source–detector separations. Figure 1 shows data for a source–detector separation of only 1 cm. After approximately 1 ns, the time-resolved signal is dominated by the optical properties of the underlying medium. In the case of a steady-state measurement, the source and the detector have to be separated by several centimeters before the underlying medium exerts a noticeable influence.[6] In many practical cases, it is not possible to separate the source and the detector significantly. Consider, for example, measurements performed through an endoscope in the gastrointestinal tract, where source–detector separations of only a few millimeters are possible. Even for measurements on relatively large objects, such as blood-oxygen-saturation measurements of the head, a large source–detector separation is not always desirable, as when the oxygen saturation is to be determined with high spatial resolution.

B. Blood-Oxygenation Determination in the Brain

The results reported so far are particularly important for the case of blood-oxygenation measurement of the brain. Here it is often desirable to detect oxygenation changes that result in a change of the blood absorption coefficient.[1–3] The skull, with a thickness of between 5 and 10 mm, has a lower absorption coefficient in the near-infrared wavelength range than does the underlying brain tissue. Let us assume that the absorption coefficient of the blood-filled brain changes from 0.2 to 0.3 cm^{-1} as a result of a change in blood oxygenation. Then, as can be seen in Fig. 5, the time-resolved reflectance measurement made on the human head gives a smaller change in the apparent absorption coefficient. Thus changes in the blood oxygenation could be underestimated.

Other factors that have been neglected so far may further influence the blood-oxygenation determination in the brain. The brain is actually encapsulated not only by the skull but also by the meninges and the skin. Besides differences in the absorption coefficients, these layers have differences in scattering coefficients. For example, the subarachnoid space, a sublayer of the meninges, is almost free of absorption and scattering. How these kinds of layers affect the time-resolved reflectance is discussed in Section 5.

5. Complex Layered Structures

A. Difference in Scattering Coefficient

In the sections above, the reduced scattering coefficients μ_s' in both layers are the same. Figure 6 illustrates the effect of an increased scattering coefficient in the top layer. Three curves generated by time-resolved Monte Carlo simulations are shown. Curve (I) corresponds to a homogeneous medium with a scattering coefficient of $\mu_s' = 5\ \mathrm{cm}^{-1}$ and an absorption coefficient of $\mu_a = 0.2\ \mathrm{cm}^{-1}$. Curve (II) belongs to the same medium with a 4-mm-thick, low-absorbing ($\mu_a = 0.01\ \mathrm{cm}^{-1}$) surface layer. As discussed above, the amplitude is increased, and after a certain time the tail of the layered system is parallel to that of the homogeneous medium. Curve

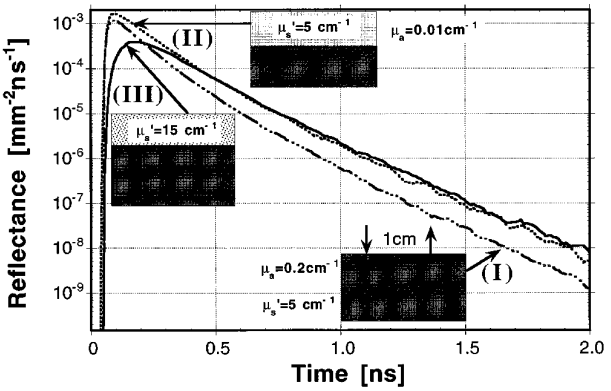

Fig. 6. Monte Carlo simulation of a two-layer system with tissues with different absorption and scattering coefficients.

(III) in the graph depicts the case in which the scattering coefficient of the upper layer is increased three times. In most biological tissues, variations in the scattering coefficient rarely exceed this difference. As can be seen in the graph, the increase in scattering leads to a smoothing of the peak in the early part of the curve. The late part of the time-resolved response is again parallel to the curve of the homogeneous underlying medium. This agrees with a statement made above that, for early times, μ_s' dominates the behavior of the reflectance signal, whereas for later times, μ_a has the stronger influence. Thus, also in this case, the absorption coefficient of the lower layer can be retrieved.

B. Multilayer Structures

The results discussed so far for two-layer systems can be generalized to multilayer systems. We first consider a three-layer system consisting of a 6-mm surface layer with a low μ_a of 0.02 cm^{-1}, an intermediate layer with a thickness of either 3 or 6 mm and a high μ_a of 0.2 cm^{-1}, and an underlying semi-infinite medium with a low μ_a of 0.02 cm^{-1}. The reduced scattering coefficients are the same throughout the medium ($\mu_s' = 9.5\ cm^{-1}$). Experimental results from this three-layer system are shown in Fig. 7. Besides the time-resolved reflectance curves from the layered-tissue phantoms, the corresponding curves for the low- and the high-absorbing homogeneous media are shown.

The curves from the layered sample first follow exactly the curve for the homogeneous medium with the same properties of the surface layer. After approximately 150 ps, the high-absorbing intermediate layer starts to exert its influence. However, after 1.5 ns, curves from the layered media again become parallel to the homogeneous medium with the same optical properties as the underlying medium. With increasing thickness of the intermediate layer, only the absolute intensity drops. These results are similar to the situation of a two-layer medium with a high-absorbing surface layer on top of a low-absorbing medium. When the average absorption coefficient of multiple top layers is higher than that of the underlying medium, the apparent absorption coefficient of the system depends primarily on the absorption coefficient of the underlying medium.

Another experimental example of a three-layer system is shown in Fig. 8. The reduced scattering coefficients are the same for all three layers ($\mu_s' = 9.5\ cm^{-1}$), whereas the absorption coefficient varies from $\mu_a = 0.2\ cm^{-1}$ to 0.02 cm^{-1} and back to 0.2 cm^{-1}. Now the top two layers have a lower average absorption coefficient than the underlying medium. Therefore the results resemble very much a two-layer system with a low-absorbing surface layer on top of a high-absorbing medium. The apparent μ_a of this system equals the μ_a of the underlying medium only if the difference in μ_a is small or if the top layer's thickness is thin.

Finally, Fig. 9 shows a Monte Carlo simulation of a three-layer system in which all layers differ in absorption and scattering coefficients. The optical properties chosen are similar to typical values for skin, skull, and brain tissues in the near infrared. The second curve in the graph corresponds to a homogeneous medium with the optical properties of the underlying medium. After 1.5 ns, the tails of the two curves become parallel, confirming once again that the lowest layer in a layered system determines in general the late part of the time-resolved reflectance.

C. Absorption- and Scattering-Free Layers

As already mentioned in Section 1, in biological tissues one also encounters layers with almost no absorption and scattering. For example, the subarachnoid space, a sublayer of the meninges, is filled with very low-absorbing and low-scattering brain fluid. We investigated the influence of such layers on time-resolved reflectance measurements.

Figure 10 shows the results of an experiment on a layered-gel phantom. Transparent pure-gel layers

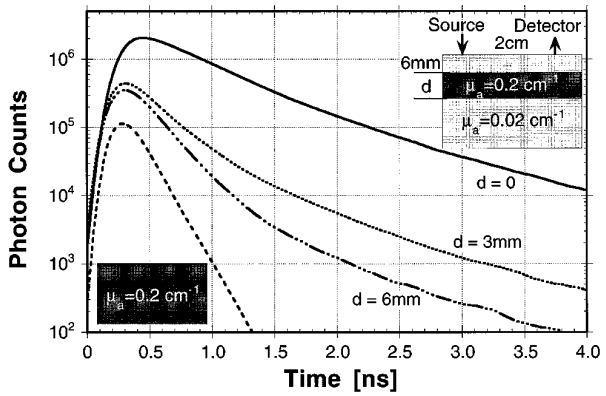

Fig. 7. Experimental results from a three-layer system in which a high-absorbing layer ($\mu_a = 0.2\ cm^{-1}$) is sandwiched between a low-absorbing 6-mm-thick surface layer and a low-absorbing underlying medium ($\mu_a = 0.02\ cm^{-1}$). The reduced scattering coefficient is kept constant at 9.5 cm^{-1}.

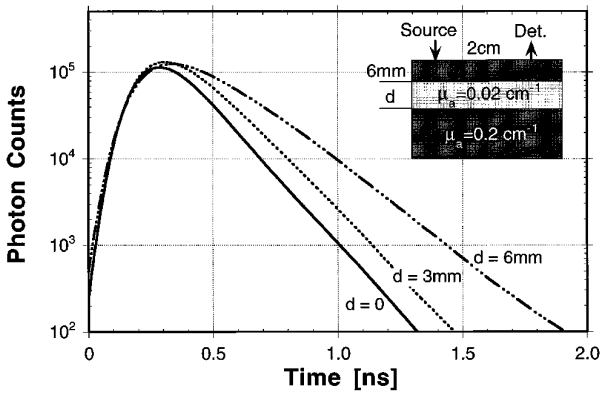

Fig. 8. Experimental results from a three-layer system, in which a low-absorbing layer ($\mu_a = 0.02\ cm^{-1}$) is sandwiched between a high-absorbing 6-mm-thick surface layer and a high-absorbing underlying medium ($\mu_a = 0.2\ cm^{-1}$). The reduced scattering coefficient is kept constant at 9.5 cm^{-1}.

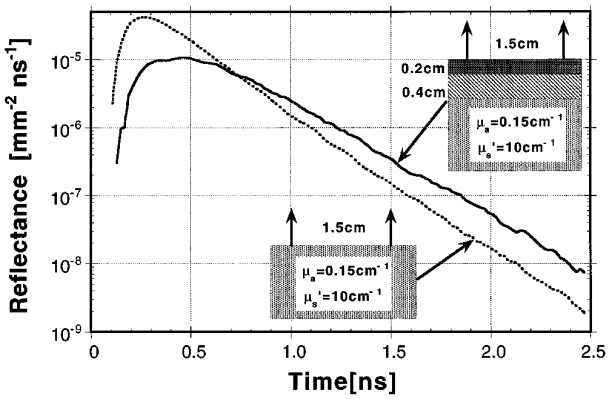

Fig. 9. Monte Carlo simulation of a multilayer system with tissues with different scattering and absorption coefficients. The top layer has coefficients $\mu_a = 0.2$ cm^{-1} and $\mu_s' = 8$ cm^{-1}, and the intermediate layer has $\mu_a = 0.05$ cm^{-1} and $\mu_s' = 24$ cm^{-1}, and the bottom medium has $\mu_a = 0.15$ cm^{-1} and $\mu_b' = 10$ cm^{-1}.

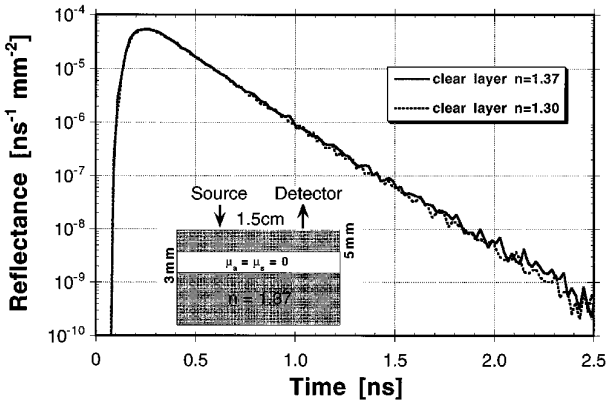

Fig. 11. Comparrision of Monte Carlo simulations of two systems. In one case (solid curve) the refractive index, $n = 1.37$, of the clear layer is the same as the one of the background medium. In the other case (dotted curve) the refractive index of the clear layer is $n = 1.30$.

with different thicknesses were sandwiched between a bulk medium with $\mu_a = 0.3$ cm^{-1} and $\mu_s' = 10.0$ cm^{-1} and a 5-mm upper layer with the same optical properties. The source–detector separation was 2 cm. As can be seen, the amplitude of the signal is increased as the thickness of the transparent-gel layer is increased. Also, the maximum position shifts slightly toward 0. However, the steepness of the decaying slope is unaffected, meaning that the apparent absorption coefficient does not change. Thus we conclude that the subarachnoid space does not affect the absorption measurements of the blood in the brain.

We also studied how a possible change in the refractive index n of the clear layer influences the time-resolved reflectance measurements. Figure 11 shows the results of two Monte Carlo simulations in which an absorption- and scattering-free 3-mm layer is sandwiched between a bulk medium with $\mu_a = 0.3$ cm^{-1} and $\mu_s' = 10.0$ cm^{-1} and a 5-mm upper layer with the same optical properties. The two simulations differ only in the refractive index of the clear layer. In one case the refractive index of the layer, $n = 1.37$, equals the refractive index of the surrounding medium; in the other case the refractive index of the clear layer is $n = 1.30$. As can be seen, the difference in the refractive index does not lead to a change of the time-resolved reflectance and, therefore, does not influence the determination of the absorption coefficient of the underlying medium.

D. *In Vivo* Measurements

As an example of how to use the knowledge acquired through simulations and measurements on gelatin-tissue phantoms, an *in vivo* measurement of the human forehead is discussed. The experiment was performed with a wavelength of 780 nm. The source–detector separation was 2 cm. The circles in Fig. 12 are the measured data, and the solid curve is a fit from diffusion theory. This fit yields an apparent absorption coefficient of 0.152 cm^{-1}. The question arises: How is this apparent absorption coefficient related to the absorption coefficient of the brain tissue?

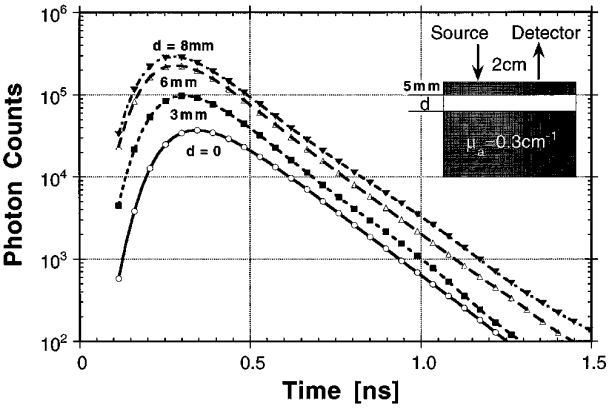

Fig. 10. Time-resolved reflectance measurements on systems containing an almost absorption- and scattering-free layer of thickness d. The refractive index $n = 1.37$ is the same throughout all layers.

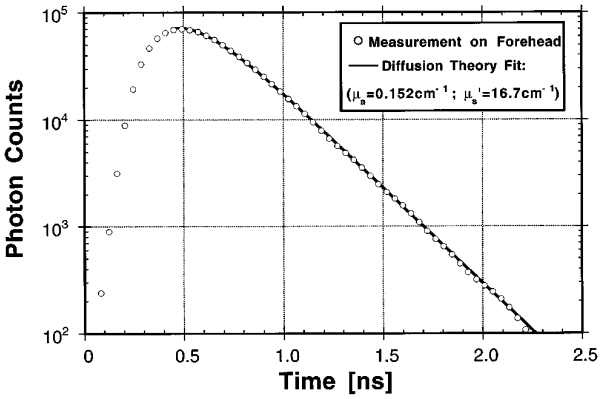

Fig. 12. *In vivo* measurement of the forehead. The source–detector separation was 1.9 cm. A wavelength of $\lambda = 830$ nm was used. Based on the results in Fig. 5, it can be concluded that the apparent μ_a determined by a diffusion-theory fit equals the μ_a of the underlying brain tissue.

We just demonstrated that the almost absorption- and scattering-free layer of brain fluid between the skull and the brain does not affect the apparent absorption coefficient. Hence this layer can be neglected. The skin on top of the skull has a higher absorption coefficient than the skull. From the above analysis of two-component structures, it is known that high-absorbing layers on top of low-absorbing layers reduce the absolute amplitude of the signal but not the shape at late times. Thus we conclude that the skin also does not influence the measurement of the absorption coefficient. What is left for consideration is the low-absorbing skull on top of the high-absorbing brain tissue. The skull on the forehead where the measurement was taken has a thickness of 5 to 8 mm. Figure 5 shows that the apparent absorption coefficient and the absorption coefficient of the underlying tissue are the same when $\mu_a = 0.152\ \mathrm{cm}^{-1}$. Thus it seems reasonable to conclude that $0.152\ \mathrm{cm}^{-1}$ is the absorption coefficient of the brain and not of the skull or any other layer encapsulating the brain. Further *in vivo* studies are needed to confirm this conclusion.

6. Summary

In our study, the influence of layered-tissue structures on time-resolved reflectance measurements was investigated numerically and experimentally. Layered gels with different concentrations of TiO_2 and india ink were used as phantoms to resemble layered-tissue structures, such as the skull encapsulating the brain. We demonstrated that, when a high-absorbing surface layer is situated on top of a low-absorbing medium, the absorption coefficient of the underlying medium can be measured. To do so, the solution of the semi-infinite time-resolved diffusion theory must be fitted to the decaying part of the response curve. The high-absorbing top layer changes only the amplitude of the recorded signal but not the shape of the later part of the curve.

When the top layer is less absorbing than the underlying medium, two regions are found. When the differences in optical properties between the two media are small, the absorption coefficient of the underlying tissue can be determined as just described. In the case of a large absorption difference between the top and the bottom media or thick top layers, the optical properties of the surface layer dominate the reflectance signal.

These results can be generalized to multilayer system as follows. When the average absorption coefficient of the top layers is higher than that of the underlying medium, the apparent absorption coefficient of the system equals the absorption coefficient of the underlying medium. In a system whose average absorption coefficient of the top layers is lower than that of the underlying medium, the apparent absorption coefficient of the system depends on the layer thicknesses and the difference in μ_a. The apparent μ_a equals the μ_a of the underlying medium only if the differences in μ_a are small or if the total thickness of the top layers is thin enough.

Furthermore, the case of an almost absorption- and scattering-free layer located between two normal tissues was examined. An important example of this kind of layer is the subarachnoid space that is filled with brain fluid. Experimental results show that such a layer gives rise to an overall increase of the signal. However, the shape of the curve is only slightly changed. The apparent scattering coefficient is decreased, while the apparent absorption coefficient is unaltered.

Applying these results to *in vivo* measurements on the human forehead, we found that the absorption coefficient of the underlying brain tissue can most likely be determined with time-resolved reflectance measurements.

The authors thank L. Wang for help in performing the Monte Carlo simulations. This work was supported in part by the U.S. Department of Energy, the Robert A. Welch Foundation, and the National Institutes of Health (R29-HL45045).

References

1. F. F. Jöbsis, "Noninvasive, infrared monitoring of cerebral and myocardial oxygen sufficiency and circulatory parameters," Science **19,** 1264–1267 (1977).
2. B. Chance, J. S. Leigh, H. Miyaka, D. S. Smith, D. S. Niola, R. Greenfeld, M. Finander, K. Kaufmann, W. Levy, M. Young, P. Cohen, P. Yoshioka, and R. Boretsky, "Comparison of time resolved and unresolved measurements of deoxyhemoglobin in brain," Proc. Natl. Acad. Sci. U.S.A. **85,** 4971–4975 (1988).
3. D. A. Benaron, W. E. Benitz, R. L. Ariagno, and D. K. Stevenson, "Noninvasive methods for estimating *in vivo* oxygenation," Clin. Pediatr. (Philadelphia) **31,** 258–273 (1992).
4. S. Takatani and M. D. Graham, "Theoretical analysis of diffuse reflectance from a two-layer tissue model," IEEE Trans. Biomed. Eng. **26,** 656–664 (1979).
5. M. Keijzer, W. M. Star, and P. R. M. Storchi, "Optical diffusion in layered media," Appl. Opt. **27,** 1820–1824 (1988).
6. R. Nossal, J. Kiefer, G. H. Weiss, R. Bonner, H. Taitelbaum, and S. Halvin, "Photon migration in layered media," Appl. Opt. **27,** 3382–3391 (1988).
7. H. Taitelbaum, S. Havlin, and G. H. Weiss, "Approximate theory of photon migration in a two-layer medium," Appl. Opt. **28,** 2245–2249 (1989).
8. J. M. Schmitt, G. X. Zhou, E. C. Walker, and R. T. Wall, "Multilayer model of photon diffusion in skin," J. Opt. Soc. Am. A **7,** 2141–2153 (1990).
9. W. Cui and L. E. Ostrander, "The relationship of surface reflectance measurements to optical properties of layered biological media," IEEE Trans. Biomed. Eng. **39,** 194–201 (1992).
10. M. S. Patterson, B. Chance, and B. C. Wilson, "Time resolved reflectance and transmittance for the non-invasive measurement of tissue optical properties," Appl. Opt. **28,** 2331–2336 (1989).
11. A. H. Hielscher, H. Liu, L. H. Wang, F. K. Tittel, B. Chance, and S. L. Jacques, "Determination of the blood oxygenation in the brain by time-resolved reflectance spectroscopy (I): Influence of skin, skull and meninges," in *Biochemical Diagnostic Instrumentation A: Optical Diagnosis of Blood and Blood Components*, B. Chance and R. R. Alfano, eds., Proc. Soc. Photo-Opt. Instrum. Eng. **2136,** 4–15 (1994).

12. S. T. Flock, B. C. Wilson, and M. Patterson, "Monte Carlo modeling of light propagation in highly scattering tissues—II: Comparison with measurements on phantoms," IEEE Trans. Biomed. Eng. **36,** 1169–1173 (1989).
13. A. H. Hielscher, L. H. Wang, F. K. Tittel, and S. L. Jacques, "Influence of boundary conditions on the accuracy of diffusion theory in time-resolved reflectance spectroscopy of biological tissues," Phys. Med. Biol. **40,** 1957–1975 (1995).
14. L. H. Wang, S. L. Jacques, and L. Zheng, "MCML—Monte Carlo modeling of light transport in multilayered-tissues," Comput. Methods Programs Biomed. **47,** 131–146 (1995).
15. S. L. Jacques, L. Wang, and A. H. Hielscher, "Time-resolved photon propagation in tissues," in *Optical-Thermal Response of Laser Irradiated Tissue*, A. J. Welch and M. van Gemert, eds. (Plenum, New York, 1995), Chap. 9.
16. L. Wang and S. L. Jacques, "Optimized radial and angular positions in Monte Carlo modeling," Med. Phys. **21,** 1081–1083 (1994).
17. I. Lux and K. Koblinger, *Monte Carlo Particle Transport Methods: Neutron and Photon Calculations* (CRC, Boca Raton, Fla., 1991).
18. D. V. O'Connor and D. Phillips, *Time-Correlated Single Photon Counting*, (Academic, Orlando, Fla., 1984).
19. H. Liu, M. Miwa, B. Beauvoit, N. G. Wang, and B. Chance, "Characterization of absorption and scattering properties of small volume biological samples using time-resolved spectroscopy," Anal. Biochem. **213,** 378–385 (1993).
20. F. A. Duck, *Physical Properties of Tissue* (Academic, San Diego, Calif., 1990), Chap. 3, 43–71.
21. V. G. Peters, D. R. Wyman, M. S. Patterson, and G. L. Frank, "Optical properties of normal and diseased human breast tissues in the visible and near infrared," Phys. Med. Biol. **35,** 1317–1334 (1990).
22. H. R. Eggert and V. Blazek, "Optical properties of human brain tissue, meninges, and brain tumors in the spectral range of 200 to 900 nm," Neurosurgery **21,** 459–464 (1987).
23. L. O. Svaasand and R. Ellingsen, "Optical properties of human brain," Photochem. Photobiol. **38,** 293–297 (1983).